Catalysis Today 195 (2012) 83–92

Contents lists available at SciVerse ScienceDirect

Catalysis Today

journal homepage: www.elsevier.com/locate/cattod

Catalyst screening for the hydrothermal gasification of aqueous phase of bio-oil

Anand G. Chakinala[a,*], Jithendra K. Chinthaginjala[a], Kulathuiyer Seshan[b], Wim P.M. van Swaaij[a], Sascha R.A. Kersten[a], Derk W.F. Brilman[a]

[a] Thermo-Chemical Conversion of Biomass (TCCB), Faculty of Science and Technology, IMPACT Research Institute, University of Twente, P.O. Box 217, 7500 AE Enschede, The Netherlands
[b] Catalytic processes and Materials (CPM), Faculty of Science and Technology, IMPACT Research Institute, University of Twente, P.O. Box 217, 7500 AE Enschede, The Netherlands

ARTICLE INFO

Article history:
Received 30 January 2012
Received in revised form 13 July 2012
Accepted 23 July 2012
Available online 27 September 2012

Keywords:
Aqueous fraction
Bio-oil
Hydrothermal
Supercritical water gasification

ABSTRACT

The catalytic gasification in supercritical water of the water soluble fraction of bio-oil, either obtained directly by phase-separated pyrolysis-oil from ligno-cellulosic biomass or by hydrotreatment of that oil, is reported in this study. Several heterogeneous metal catalysts Pt, Pd, Ru, Rh, and Ni supported on alumina were tested for their gasification efficiency (GE). The GE for the metals is decreasing in the order Ru > Pt > Rh ~ Pd > Ni. For optimum H_2 selectivity the order of the catalysts is Pd > Ru ~ Rh > Pt > Ni. Pd catalysts with different supports have been screened and no significant changes in the GE were found for the different supports. However, the composition of the product gas differed significantly with the support type. High H_2 selectivity was obtained with Al_2O_3 and Ce–ZrO_2 supports. With increasing the organic concentration from 5 to 50 wt% the GE as well as the H_2 and CO_2 selectivities dropped significantly. High reaction temperatures, long residence time, low feed stock concentrations and high catalyst loadings favored the high carbon to gas conversion. The aqueous wastes streams obtained from the hydrodeoxygenation process for the pyrolysis oil are easier to reform in supercritical in comparison to the feedstocks obtained directly as pyrolysis condenser fraction or as phase-separated aqueous fraction. Complete conversion of the made-up and the fast pyrolysis condenser fraction was obtained at low feed concentrations (5 wt%) using a continuous flow reactor in the presence of Ru/Ce–ZrO_2 catalyst. However, the catalyst quickly deactivated with the made-up fraction but the same catalyst retained its stability and activity with the pyrolysis condenser fraction during the 3 h test run. The supercritical water gasification seems therefore a very suitable step for treating the aqueous phase obtained after hydrotreatment of pyrolysis oil in a (biomass) refinery concept.

1. Introduction

Bio-fuels derived from renewable biomass sources are one of the promising candidates for sustainable energy production, predominantly those based on agricultural/forestry residues and on waste streams. Using a thermo-chemical conversion method to convert the biomass into bio-fuels, the option exists to produce either a gaseous or liquid fuel. However, there are several techno-economic challenges associated with these conversion processes to do this in a cost effective way, particularly, when converting aqueous waste biomass streams containing 80% water or more. Such low calorific value waste effluents can be converted into a higher heating value product gas either by aqueous phase reforming [1] (APR) or via supercritical water gasification (SCWG; above 374 °C and 221 bar) [2–7].

Several researchers have studied the catalytic gasification of real biomass such as wood [4], algae [3] in hot compressed water. Waldner and Vogel [4] have reported the complete conversion of wood sawdust by catalytic hydrothermal gasification at 400 °C and 340 bar with Raney nickel catalyst using very long reaction times (1–2 h). They obtained a maximum methane selectivity corresponding to the thermodynamic equilibrium predictions. However, during the continuous operation of synthetic liquefied wood (mainly consisted of formic acid, acetic acid, ethanol, phenol, and anisole) gasification at 400 °C and 300 bar, Raney nickel was reported to exhibit high initial activity but sintered rapidly, accompanied with loss of metal surface area. Addition of metals such as Ru, Fe, Mo or Cu had no influence on the activity and stability (the ability to maintain its activity for a long period of operation) of the Raney nickel. However, when supported on carbon, Ru catalyst was reported to be more stable and active for 220 h even at high feed concentrations of the synthetic liquefied wood and space velocities [6].

Virtually, the real biomass streams in its original state (consisting of irregular size, minerals chemically bounded with inherent contaminants to the biomass, mixed with sand, etc.) are not suitable for processing in supercritical water and therefore needs a pretreatment step such that the homogenous slurries can be fed to the

* Corresponding author. Tel.: +31 53489 4635; fax: +31 53489 4738.
E-mail address: a.g.chakinala@gmail.com (A.G. Chakinala).

0920-5861/$ – see front matter © 2012 Elsevier B.V. All rights reserved.
http://dx.doi.org/10.1016/j.cattod.2012.07.042

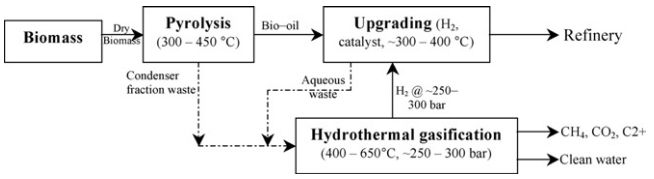

Fig. 1. Conceptual bio-refinery process with integrated hydrothermal gasification for hydrogen production from aqueous wastes produced.

reformer. One way of processing the raw, inhomogeneous feed is to use biomass flash pyrolysis, in which dry biomass is converted by rapidly heating (300–500 °C) in the absence of oxygen and by condensing the vapors produced, thereby obtaining a liquid product called bio-oil or pyrolysis oil (~60–75% selectivity on weight basis, depending on the operating parameters and condenser fractions) [2,5]. Bio-oil can be steam reformed [8,9] to produce synthesis gas (syn-gas) which can further be upgraded by Fisher–Tropsch synthesis or the bio-oil itself can be upgraded directly by catalytic hydrogenation/hydro deoxygenation to reduce the oxygen content, making the product viable for co-processing in an oil refinery [10]. Fig. 1 illustrates a conceptual scheme integrated with hydrothermal gasification of aqueous wastes derived in a bio-refinery for hydrogen production.

In this paper, bio-oil was phase-separated into an aqueous and a non-aqueous fraction by addition of water. The aqueous fraction of bio-oil thus obtained was catalytically reformed in supercritical water using a batch autoclave reactor. Till date, very little work has been reported on the hydrothermal gasification of a highly diluted aqueous fraction of bio-oil. Penninger and Rep [2] reported the supercritical water gasification of aqueous wood condensate (<4% organics in water) in a tubular flow reactor and obtained H_2 rich product gas at 650 °C and 280 bar with a carbon to gas conversion of about 90%. Addition of low concentrations of soda (<0.1% Na_2CO_3) promoted the water–gas shift (WGS) reaction resulting in high H_2 selectivities. However, increasing the organic concentration caused tar formation and as a consequence led to reactor plugging. Di Blasi et al. [11] have reported the supercritical water gasification of wastewater collected (diluted with pure water to initial TOC concentrations of 6.5–31 g/L) at the downstream of an updraft wood gasification plant at temperatures in the range of 450–548 °C and they obtained TOC conversions in between 30 and 70% with an activation energy of 76 ± 22 kJ/mol and pre-exponential factor $897 \pm 30\ s^{-1}$. They found difficulty in gasifying high feed concentrations of wastewater which led to clogging at the outlets of the pump. Vispute and Huber [1] have reported the aqueous phase reforming (APR) of the water soluble fraction of pyrolysis oil containing 1 wt% organics at 265 °C and 55 bar with Pt catalyst and obtained a carbon to gas conversion of 35% and alkane selectivity of 45% at a WHSV of $0.96\ h^{-1}$. Byrd et al. [7] have screened several catalysts for the hydrogen production from switch grass bio-crude (1.0–1.3 wt% of carbon) in supercritical water (600 °C; 250 bar) and they observed very quick reactor plugging due to severe coke formation with almost all the catalysts studied associated with significant loss in surface area of the catalysts due to sintering. To conclude, very few studies have addressed the practical problems that are encountered in supercritical water gasification of real biomass slurries such as reactor plugging and incomplete conversion of realistic feedstock. Idesh et al. [12] have screened several nickel supported on carbon catalysts for the reforming of water soluble fraction (initial TOC content of the organics was 10,000 ppm) of biomass pyrolysis oil in a continuous reactor and found that the Pt impregnated on Ni catalysts was active and stable for 24 h duration test at 350 °C and 200 bar.

The aim of this work is to develop an efficient catalyst to completely convert the aqueous phase of bio-oil (~18% organics) in SCW. The design criteria for the catalyst development are to achieve (i) complete carbon to gas conversion, (ii) tune the product gas selectivity towards hydrogen and (iii) minimize char/coke formation that usually leads to reactor plugging in a continuous flow reactor. Catalyst screening involving the influence of different metals, supports and also reaction parameters (e.g., temperature, feed concentration, residence time, feed nature) on the gasification behavior were probed.

2. Experimental methods

2.1. Materials

γ-Alumina (γ-Al_2O_3, BASF), activated carbon (AC, Norit ROX 0.8), silica (SiO_2, Evonik), zirconia (ZrO_2, Evonik), titania (TiO_2, Evonik) were used as catalyst supports. Cerium nitrate hexahydrate was also used as catalyst deposited on zirconia support. Acetylacetonate salts comprising of Pt, Pd, Ru, Rh and Ni were used in the preparation of respective metal catalysts.

2.2. Catalyst preparation and characterization

The catalyst supports were pulverized to particle size ranging between 300 and 600 μm. Organic phase wet impregnation method was used to deposit active metal on the surface of the support using the respective metal acetylacetonate precursor dissolved in toluene. The supports were immersed in toluene, containing the proper amount of metal precursor dissolved, in a round bottomed flask of a vacuum rotary evaporator. The flask was immersed in silicon oil bath maintained at a temperature of 45 °C. Toluene was completely evaporated by slowly applying vacuum and leaving behind the metal precursor deposited on the support. The respective catalysts were obtained by decomposing the metal precursor deposited on supports by calcination in air at 300 °C (ramp of 5 °C/min) for 2 h and at 600 °C (ramp of 5 °C/min) for 1 h and subsequently the samples were reduced at 600 °C for 1 h and then and then cooled to room temperature. Similar conditions were followed for all the catalysts except for the preparation of Pd supported on activated carbon, where the sample was calcined at 250 °C (ramp of 5 °C/min) for 2 h and then reduced at 550 °C (ramp of 5 °C/min) for 1 h and then cooled to room temperature.

In the preparation of metal (Ru, Pd) supported ceria–zirconia (here after denoted as Ce–ZrO_2) catalysts, the required amounts of cerium nitrate hexahydrate precursor were dissolved in water and then dispersing zirconia particles in the solution, in a round bottomed flask of a vacuum rotary evaporator. The flask was immersed in silicon oil bath maintained at a temperature of 75 °C. Water was completely evaporated by slowly applying vacuum and leaving behind the Ceria precursor deposited on the zirconia particles. The support was then calcined in air at 600 °C (ramp of 5 °C/min) for 6 h and then cooled to room temperature at ramp of 10 °C/min. The Ce–ZrO_2 support was then deposited with respective metal acetylacetonate precursor by following the procedure mentioned above.

Table 1 presents the details of all the catalysts used in this study. It is clear from the table that activated carbon possess the highest surface area among all the supports and the order of the support with respect to BET surface area is AC > γ-Al_2O_3 > SiO_2 > ZrO_2 ~ TiO_2 ~ Ce–ZrO_2. Since it is difficult to prepare all the catalysts having similar loadings and similar particle sizes, the particle sizes and metal loadings shown in Table 1 are different.

X-ray fluorescence spectroscopy (XRF) (Phillips PW 1480 spectrometer) was used to determine the catalyst composition. The active metal particle size was determined by CO chemisorption. The BET surface area and porosity of all the catalysts were

Table 1
Characteristics of the fresh catalysts used in the experiments.

Catalyst type	Metal loading (wt %)	Active particle size (nm)	BET surface area (m^2/g)
$Pt/\gamma\text{-}Al_2O_3$	3.32	3	N.D.
$Ni/\gamma\text{-}Al_2O_3$	2.92	221	N.D.
$Rh/\gamma\text{-}Al_2O_3$	2.32	N.D.	N.D.
$Pd/\gamma\text{-}Al_2O_3$	2.51	5	199
$Ru/\gamma\text{-}Al_2O_3$	2.41	111	N.D.
Pd/TiO_2	1.27	36	44
Pd/ZrO_2	1.93	11	45
Pd/SiO_2	1.80	7	166
Pd/AC	1.88	174	1146
$Pd/Ce\text{–}ZrO_2$	Pd = 1.57 Ce = 7.77	N.D	45
$Ru/Ce\text{–}ZrO_2$	Ru = 0.97 Ce = 10.7	N.D.	45

N.D. – not determined.

determined using with nitrogen adsorption–desorption at −196 °C in a Micromeritics TriStar instrument. The crystal structures of the fresh and spent catalysts were analyzed by powder X-ray diffraction (XRD) performed on a Philips X'pert device with CuKα as the radiation source. Step scans were taken in the range 2θ from 15 to 75°. Due to the limitations of XRD sensitivity, a minimum of ∼5 wt% metal loading sample is needed for identification and quantification of the crystallite size using the Scherrer equation. Thermogravimetric analysis (TGA) of the spent catalysts was carried out in alumina crucible using NETZSCH STA 449 F3 Jupiter instrument. The samples were heated from room temperature to 850 °C at a heating rate of 10 °C/min in a stream of flowing air (30 ml/min). The samples were held at 850 °C for 30 min to completely oxidize the carbonaceous deposits. The initial mass of the samples was determined using an external weighing balance. The mass rate loss is defined as

$$r_{wt} \equiv \frac{dX}{dT} = -\frac{(m_\tau - m_{\tau+1})}{m_0(T_\tau - T_{\tau+1})}(1/^\circ C)$$

where τ and $\tau+1$ are logged time, T (°C) is the temperature of the sample cup and m_o (mg) is the initial amount of sample, as weighed with the external balance.

2.3. Feed stock analysis

Three different feedstocks: (i) made-up fraction, (ii) pyrolysis condenser fraction [13,14] and (iii) hydro-deoxygenation fraction (HDO) [15] were used in this study. The feedstocks characteristics are given in Table 2. The made-up organic fraction-I and II were prepared by mixing pyrolysis oil produced by VTT (Finland) from forest residue [9,10,15] and water in 1:2 and 1:1 ratios respectively to induce phase separation and to obtain a desired organic concentration. The pyrolysis oil and water mixture was phase separated over night in a conical funnel and the water soluble fraction of organics in the bio-oil was filtered with a Whatman filter paper which is then used for the experiments.

The pyrolysis condenser fraction was obtained from the second condenser which is operated at room temperature by pyrolyzing pine wood at an oven temperature of 480 °C in our laboratory scale pyrolysis plant (1 kg/h) which is described elsewhere [14,16,17].

The aqueous HDO fraction was obtained from the HDO experiments with pyrolysis oil produced by VTT (Finland) from forest residue in a batch autoclave reactor in the presence of Ru/C catalyst and more details of this set-up are described elsewhere [10,15]. However, we could not trace back the exact experimental conditions of the HDO fraction obtained, the type of compounds present in the HDO fraction are still comparable with literature as well as our own work.

Karl–Fischer titration was used to determine the water content of the feedstocks used in this study. The elemental composition of the wet feedstocks used in the experiments was analyzed using a CHNO elemental analyzer (Fisions Instruments 1108 EA CHN-S). The composition on a dry water free basis for different feedstocks is shown in Table 2.

Table 2
Feedstock characteristics.

Aqueous fraction ID	Organics (wt%)	H_2O[a] (wt%)	Elemental composition (%)		
			C	H	O
Made-up-I	18.4	81.6	47.39	5.62	46.99
Made-up-II	51.5	48.5	47.38	3.52	49.10
Pyrolysis condenser	17.5	82.5	47.82	5.35	46.84
Hydro-deoxygenation	23.0	77.0	51.02	3.89	45.09

[a] Analyzed with Karl Fisher titration.

2.4. Experimental set-up and procedure

The catalytic hydrothermal gasification of the aqueous fraction of bio-oil was conducted in a "home made" batch autoclave reactor, having an internal volume of 45 ml, and is shown in Fig. 2. For safety reasons, the reactor set-up was placed in a high pressure box and is controlled automatically from outside the room during the experiments. The reactor lid had two orifices, one for a thermocouple and another one to connect it to a line with a pressure indicator and a gate valve. The pressure and the temperature of the reactor could be recorded and monitored with Pico Log software. With the help of a pneumatic arm, the autoclave could be immersed into and removed out of the fluidized sand bed after the reaction. This sand bed was heated by an electric oven (with preheated fluidization gas).

The experimental procedure was as follows: in a typical run, ∼4.5 g of aqueous feed solution and 0.5 g of catalyst (depending on the experimental condition) was loaded into the reactor then closed tightly and connected to the pneumatic arm of the set-up. The elemental composition of the aqueous fractions of bio-oil is given in Table 2. The line with the pressure reader was connected to the autoclave and flushed with nitrogen several times to remove any oxygen present in the system. The reactor was then pressurized with 20 bar of nitrogen which served the purpose for a leak test. The line connecting to the autoclave was removed and the high pressure safety box was closed and the remainder of the experiment was monitored from outside. Using the pneumatic arm, the autoclave is positioned on the fluidized sand bed and then the reaction was initiated by immersing the autoclave with the help of a piston into the preheated fluidized sand bed which had a temperature of ∼30 °C higher than the desired reaction temperature. After the desired reaction time, the reactor was lifted and quenched in a cold water bath. The heating-up time of the reactor was around 5 min to reach the reaction conditions.

Gas samples were taken in a syringe and analyzed using a micro gas chromatography (Varian CP 4900; 10 mmol sieve 5A Ar, 10 mmol sieve 5A He, 10 m PPQ He, 8 m Sil-5CB He) used to detect H_2, O_2, N_2, CH_4, CO, CO_2, C_2H_4, C_2H_6, C_3H_6 and C_3H_8. With the gas composition, the final pressure and temperature inside the reactor, the amount of each gas produced was calculated. After the reactor was cooled, it was depressurized and the autoclave was disconnected from the arm and opened. The remaining products (liquid and solids in suspension) were collected in a glass bottle and the reactor was rinsed with acetone to remove any water-insoluble deposits. The aqueous phase was analyzed for dissolved organic carbon with an elemental analyzer. Since the carbon content in the liquid effluent after the reaction was very low these values are therefore not given.

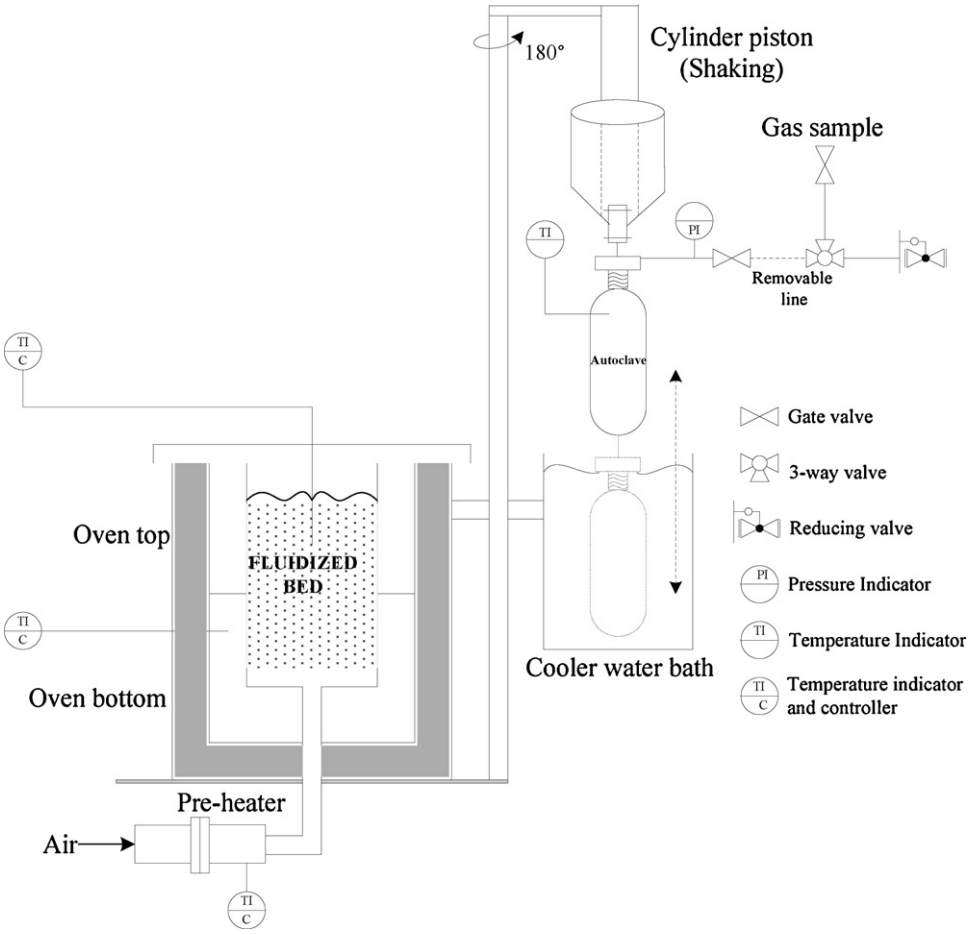

Fig. 2. Schematic diagram of the experimental batch autoclave reactor set-up.

2.5. Chemical equilibrium

Chemical equilibrium calculations were obtained using an in-house developed Matlab program that calculates according to the Gibbs minimization method [18] and the fugacity coefficients were calculated with the modified Soave–Redlich–Kwong (SRK) equation of state [19]. The parameters for the modified SRK equation of state were obtained from Bertucco and Soave [20,21]. Thermodynamic properties were obtained from NIST-JANAF source. The equilibrium program calculates the yield (mol gas/mol feed) of permanent gases (H_2, CO, CO_2 and CH_4) and the yields of C_2—C_3 compounds are neglected in this program as their values are considered to be very small. The gas yields are used to calculate the selectivities.

2.6. Continuous set-up

Details of the continuous set-up used for the catalytic reforming of aqueous fraction of bio-oil are described in our article [22].

2.7. Terms and definitions

The gasification efficiency (GE) or carbon to gas conversion is defined as the degree of conversion of carbon in the feed to "C" containing gases.

$$\text{Gasification efficiency, GE}(\%) = \frac{\sum_i N_{c,i}}{N_{c,feed}} \times 100$$

The H_2 selectivity is defined as (H_2 moles produced/C atoms in gas phase) (1/RR) × 100, the reforming ratio (RR) is 1.97, 1.75 and 1.38 for the made-up fraction, pyrolysis condenser fraction and the HDO fraction respectively.

Selectivity of carbon containing compounds *i*, % = (C atoms in species *i*)/(C atoms in gas phase) × 100, where species *i* = CO, CO_2, CH_4 and C2+ (C_2H_4, C_2H_6, C_3H_6, C_3H_8). The alkane selectivity reported is the sum of methane and higher alkanes.

The amount of catalyst loading is defined as grams of catalyst per grams of dry organics ($g_{catalyst}/g_{dry\ organics}$).

3. Results and discussion

Here we present the results of the influence of different noble metals, supports and parametric evaluation such as temperature, residence time, feed stock concentration and different kinds of feeds on the carbon to gas conversion and product gas selectivities. Finally, post-mortem analyses of the spent catalyst characterization results are discussed.

3.1. Equilibrium composition

Thermodynamic chemical equilibrium values were calculated using a Matlab program as described previously [3,22]. Fig. 3 displays the equilibrium composition of the SCWG of water soluble fraction of bio-oil (18% organics) as a function of temperature. Increasing the reaction temperature has a significant effect on the product gas distribution. The H_2 selectivity increases and CH_4 selectivity decreases significantly, while the temperature effect on CO_2

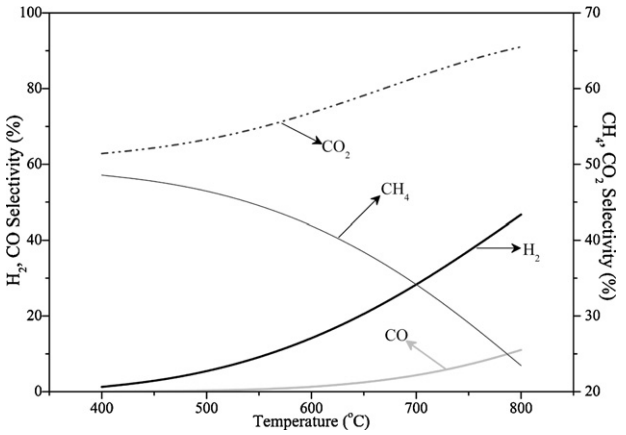

Fig. 3. Thermodynamic equilibrium gas composition of the SCWG of aqueous fraction of bio-oil ($CH_{1.36}O_{0.71}$ 18% organics) at 300 bar and different reaction temperatures.

and CO selectivity is less pronounced and only a marginal rise in the selectivity is noticed upon increasing the temperature above 600 °C. At near critical temperatures methane and carbon dioxide are the major products. At 500 °C, methane is still the main product with a selectivity of 46.5% (mole CH_4/mole C in feed) whereas the H_2 selectivity is about 5.4%.

3.2. Effect of different noble metal catalysts

The carbon gasification efficiency and product gas selectivities (H_2, CH_4, higher alkanes) of aqueous bio-oil gasification in SCW at 500 °C and 280 bar for 15 min of reaction time and in the presence of various transition metal (Pt, Ru, Pd, Rh, Ni) catalysts supported on γ-Al_2O_3, is shown in Fig. 4. The product composition and the gasification efficiencies were significantly different with different metals. All the catalysts except Ni showed reasonable carbon to gas conversions. The highest gasification efficiency was achieved with Ru catalyst (%) and the order of the catalysts in terms of conversion is Ru > Pt > Rh ∼ Pd > Ni. Palladium catalyst showed higher selectivity towards H_2 and the order of the catalysts in terms of H_2 selectivity are Pd > Ru ∼ Rh > Pt > Ni. Ru catalyst showed significantly high selectivity towards methane. The plausible reactions for the formation of alkanes can be due to the dehydration reaction of the oxygenated compound, Fischer–Tropsch synthesis or via methanation reaction. The order of the catalysts in terms of CH_4 selectivity is Ru > Rh > Pt > Pd > Ni. These trends suggest that an effective catalyst for the reforming of oxygenated compounds would be based on metals that generally possess high activities towards C—C bond breaking [23,24], which is required to obtain gaseous "C" specie (in the form of CO, CO_2, CH_4) from the oxygenated compound and high water–gas shift activity.

The presence of active metals not only influences the carbon to gas efficiencies but affects the product gas distribution. High H_2 selectivity is favored upon the active metals which show low methanation activity and low hydrogenation activity. The high methanation activity of Ru found is in agreement with the literature [23,24]. For Pd and Pt reasonable GE and hydrogen selectivity are obtained. Davda et al. [23,24] also reported high H_2 selectivity over Pd catalysts for the aqueous phase reforming of ethylene glycol. Ni based catalysts are very attractive as they are readily available and cost effective when compared to noble metal catalysts, despite their methanation activity and least stability in the SCWG process. The nickel catalyst was found to be least active among all the catalysts studied which is due to very less metal loading, leading to the formation of stable $NiAl_2O_4$ during the calcination process. Catalysts with higher Ni loadings usually present in two phases, NiO accompanied with stable $NiAl_2O_4$. The NiO phase is easily reducible with the in situ generated hydrogen during the reforming process. While, the stable $NiAl_2O_4$ phase do not contribute to any reforming activity unless it is reduced with hydrogen at high temperatures (∼800 °C) [22]. Thus, the low activity of the Ni catalysts compared to other catalysts is due to the presence of Ni in inactive and stable $NiAl_2O_4$ phase, in this case.

To conclude Pd catalysts showed reasonable gasification efficiencies with high H_2 and low alkane selectivity, while Ru catalysts exhibited higher conversion with low H_2 and high alkane selectivities. In view of these observations further catalyst screening studies have been performed with Ru and Pd metal catalysts.

3.3. Effect of different support materials

In view of the reforming activity of Pd supported on alumina catalyst (high H_2 and low alkane selectivities) when compared to other metal catalysts as discussed earlier, various Pd catalysts were prepared to study the influence of the support materials on the activity and the hydrogen production selectivity by reforming the water soluble fraction of bio-oil in supercritical water. Fig. 5 illustrates the effect of various supported Pd catalysts on the GE and product gas selectivities of aqueous fraction of bio-oil (18% organics) reforming at 500 °C, 280 bar and 15 min of reaction. For the Pd/support combinations studied, all catalysts showed similar GE. Both ZrO_2 and Al_2O_3 supported Pd catalysts showed high selectivity towards H_2. γ-Al_2O_3 is widely used as a catalyst support for a variety of process including the SCWG applications, owing to its high specific surface area, high thermal stability and low cost. Water gas shift activity is essential to increase the H_2 selectivity. It was reported that supports with red–ox properties such as TiO_2, ZrO_2 and CeO_2 can effectively enhance the shift activity [25]. Basic supports are shown to be more stable than γ-Al_2O_3 and have a higher selectivity towards hydrogen than alkanes in biomass gasification [26]. Altering the red–ox properties of the support and surface oxygen mobility is a way to enhance the catalyst performance. Ceria is as an oxide support possessing high red–ox properties and the mobility of surface oxygen/hydroxyl groups. Reduction of Ce^{4+} to Ce^{3+} aids in the formation of bridging hydroxyls, which are claimed to be active for WGS reaction [25]. Mixed oxides of Ce–ZrO_2 promote the red–ox properties of the support and are shown to have improved the catalyst performance in the WGS reaction [25,27,28]. In this study, among the Pd based catalysts, Ce–ZrO_2 support indeed showed high selectivity towards H_2, which makes it a promising support for effective shift activity under these conditions. For the reforming of switch grass bio-crude in SCW a lower GE was observed for the titania supported catalysts whereas a high hydrogen selectivity was reported with ZrO_2 supported catalysts [7]. Several researchers have studied the influence of support on the catalytic activity in hydrothermal gasification of biomass [29–31]. Minowa and Ogi [26] have studied the hydrothermal gasification of cellulose in a batch autoclave reactor using reduced nickel catalysts with different supports and they report a strong influence of supports on the catalytic activity in terms of product gas selectivities which is attributed to the acidity/basicity of the supports but also depended on the overall catalyst size (BET surface area) and active metal particle size (nickel crystallite size).

Apparently, Ce–ZrO_2 is a promising support due to the aforementioned reasons in terms of enhanced WGS activity as well as high stability to withstand under hydrothermal conditions. Therefore, further optimization studies have been carried out either with Pd or Ru metal catalysts.

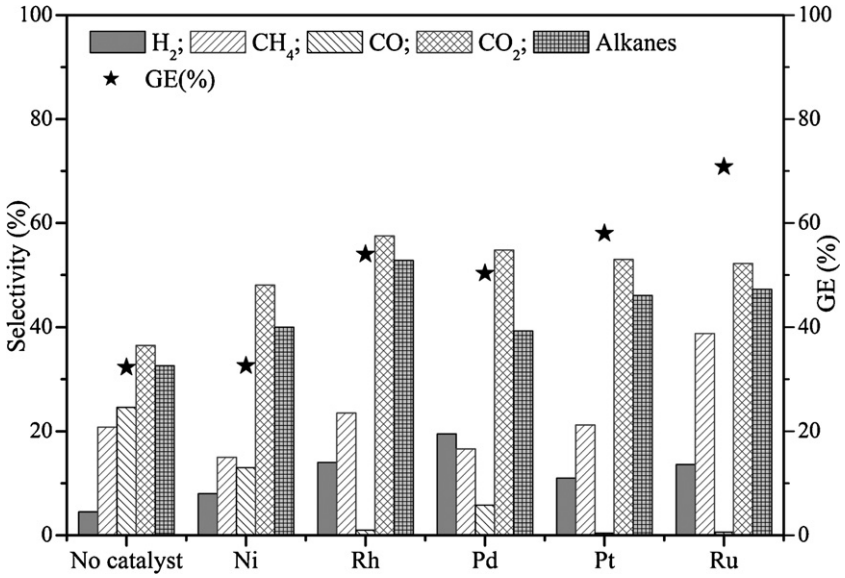

Fig. 4. The influence of different noble metal catalysts supported on alumina on the carbon to gas conversion and product gas selectivities of aqueous bio-oil (Made–up–I) reforming in SCW at 500 °C, 300 bar, 15 min reaction time and a catalyst loading of 0.6 ($g_{catalyst}/g_{dry\ organics}$).

3.4. Effect of temperature

It is well known that higher temperatures enhance the gasification efficiency and according to equilibrium calculations hydrogen selectivity is favored. The effect of temperature ranging from 450 to 580 °C on the activity and product gas selectivities of 18 wt% organics at 300 bar and 15 min of reaction time with Ru and Pd supported on Ce–ZrO_2 is shown in Fig. 6. Both the catalysts (Ru and Pd) show considerable increase in the GE with increase in temperature. Ru showed better GE over Pd at all temperatures. CH_4 selectivity with both the catalysts increases with the increase in temperature. Higher alkane (C_2, C_3) selectivity increases with temperature over Pd and Ru. Methanation activity of both the catalysts increases with temperature, however, Pd shows low methanation activity as compared to Ru. At high temperature Pd showed high H_2 selectivity and reasonably high activity. The selectivity towards CO was very low with both the catalysts.

3.5. Effect of reaction time

Generally, increasing the contact time or residence time of the reactant with the catalyst increases the conversion and steer the product gas selectivity towards equilibrium. The effect of residence time on the activity of Ru supported on Ce–ZrO_2 and product gas selectivities of 18% organics aqueous bio-oil feed at 580 °C is shown in Fig. 7. It is evident from the figure that an increase in the reaction time led to slight increase in the GE. No significant changes in the product gas selectivities are observed except for marginal changes in the hydrogen selectivity which decreases slightly after 15 min of reaction time.

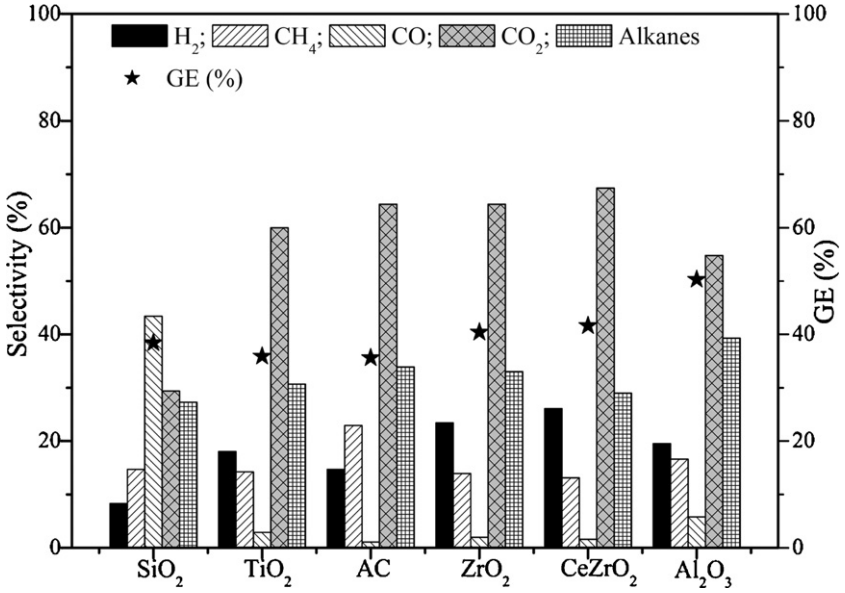

Fig. 5. The influence of different palladium supported catalysts (silica, titania, activated carbon (AC), zirconia, ceria–zirconia, γ-alumina) on the carbon to gas conversion and product gas selectivities of aqueous bio-oil (Made-up-I) reforming in SCW at 500 °C, 300 bar, 15 min reaction time and a catalyst loading of 0.6 ($g_{catalyst}/g_{dry\ organics}$).

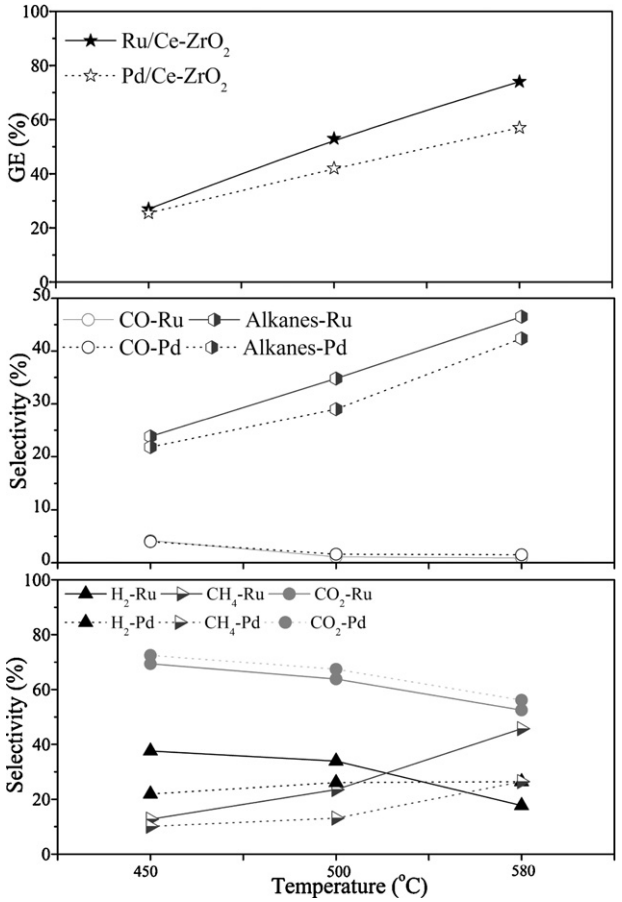

Fig. 6. The influence of different temperatures on the carbon to gas conversion and product gas selectivity of aqueous bio-oil (Made-up-I) reforming in SCW at 300 bar, 15 min reaction time, catalyst loading of 0.6 ($g_{catalyst}/g_{dry\ organics}$), Ru/Ce–$ZrO_2$ (solid trend lines), Pd/Ce–ZrO_2 (dotted trend lines).

3.6. Effect of catalyst loading

High catalyst loadings generally increase the rate of reaction due to the availability of large number of active metal particles that accelerates the carbon conversion. The influence of three different Ru/Ce–ZrO_2 catalyst loadings ($g_{cat}/g_{organics}$) on the activity and H_2, CH_4 selectivities at 580 °C and 15 min reaction time is shown in Fig. 8. H_2 selectivity decreased with increasing catalyst loading while no significant change in the alkane selectivity was noticed. Maximum carbon to gas conversion was observed at the highest catalyst loading, but a further increase in catalyst loading is expected to have little effect (Fig. 8). Elemental analysis of the liquid effluent after the reaction at higher conversions indicated almost no carbon present and this incomplete carbon balance closure can be attributed to the formation of coke either during the heating up period or the reaction.

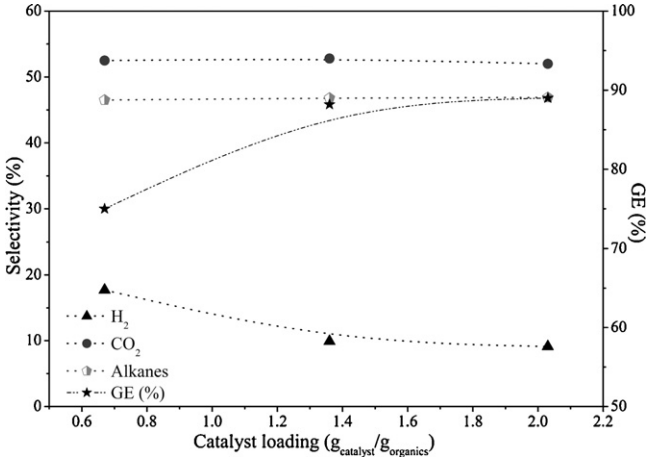

Fig. 8. The influence of Ru/Ce–ZrO_2 catalyst loading on the carbon to gas conversion and product gas selectivity of aqueous bio-oil (Made-up-I) reforming in SCW at 580 °C, 280 bar and 15 min reaction time.

3.7. Effect of organic concentration

High feed stock concentrations are beneficial both from process and economics point of view and it is shown that the net process energy efficiency of the SCWG improves with high feed stock concentration of biomass [32,33]. The influence of three different concentrations of aqueous fraction of bio-oil (9, 18 and 50 wt%) on the reforming activity of the selected Pd/Ce–ZrO_2 catalyst at 500 °C and 15 min reaction time is depicted in Fig. 9. In line with trends reported earlier, the GE decreased significantly with increasing feed concentration. Maximum conversion was achieved at the lowest concentration (9 wt% feed concentration). The H_2 and CO_2 selectivities decreased with increasing feed concentration, while a marginal increase in alkane selectivity was noticed.

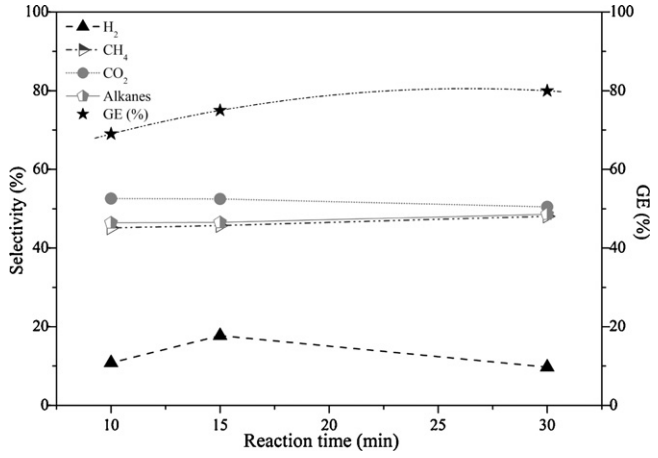

Fig. 7. The influence of reaction time on the carbon to gas conversion and product gas selectivity of aqueous bio-oil (Made-up-I) reforming in SCW at 580 °C, 300 bar, catalyst loading of 0.6 ($g_{catalyst}/g_{dry\ organics}$) of Ru/Ce–$ZrO_2$.

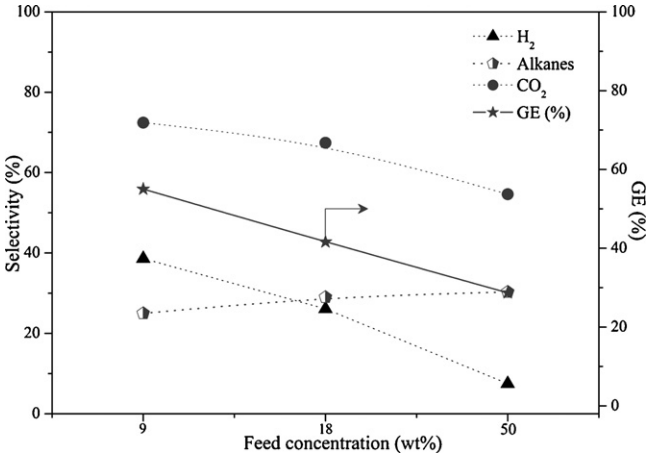

Fig. 9. The influence of different feed concentrations of aqueous bio-oil on the carbon to gas conversion and product gas selectivities in supercritical water at 500 °C, 280 bar, 15 min reaction time and Pd/Ce–ZrO_2 catalyst (0.5 g).

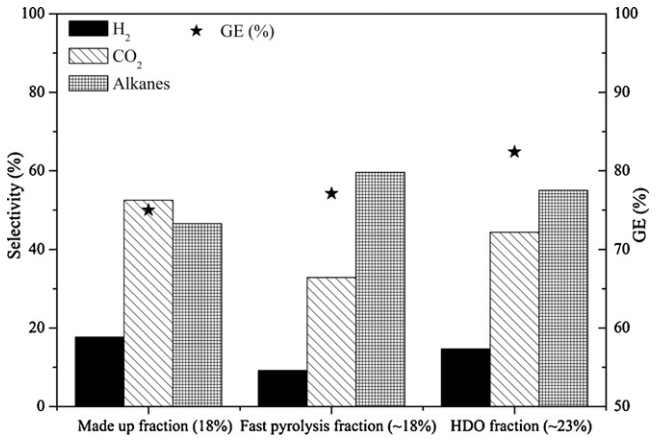

Fig. 10. The influence of different aqueous bio-oil feedstocks on the gasification behavior in supercritical water at 580 °C, 280 bar, 15 min reaction time and Pd/Ce–ZrO_2 catalyst.

3.8. Nature of the feed

Generally, the characteristics of feedstocks have a significant influence on the gasification behavior in supercritical water. The influence of different feedstocks (refer to Table 2) was tested with the Pd/Ce–ZrO_2 catalyst at 580 °C and 15 min reaction time and the results are shown in Fig. 10. Notable differences in GE and product gas selectivities are noticed for the different feedstocks. These differences in the GE can be due to the organic compounds present in the feedstocks. This is likely to be due to the presence of dissolved sugars (levoglucosan) and refractory components that are present in the phase separated made up fraction and not in the fast pyrolysis condensate and the HDO fraction [15,16]. These sugar-compounds are very reactive leading to char formation which eventually reduces the gas production and are hence liable for a lower carbon to gas conversion.

Comparatively, less GE was obtained with the made-up bio-oil fraction than with the other two feed stocks. Even though, the HDO fraction has the highest feed concentration of organic material, it has slightly the highest conversion, primarily due to the nature of the organic compounds. During the HDO process, the sugars present in the pyrolysis oil are hydrogenated in the presence of a catalyst to their respective sugar alcohols (polyols) [1], which are easy to reform and has much lesser tendency towards coke formation. The H_2 and CO_2 selectivities were reduced while the alkane selectivity increased with the fast pyrolysis fraction and the HDO fraction when compared with the made up fraction.

Fig. 11 presents the gasification efficiency and the product gas selectivities of catalytic reforming of the made-up fraction and the fast pyrolysis condenser fraction in supercritical water using a continuous flow reactor. It is noteworthy, that very low initial feed concentrations were used in the continuous flow reactor to avoid any reactor plugging due to char/coke formation at high feed concentrations. It is evident from figure that complete conversion was obtained with the pyrolysis condenser fraction during the 3 h with stable product gas selectivities. Relatively, less conversion was obtained with the made-up fraction and the selectivity towards C2 compounds is seen after 2 h as well as the liquid effluent turned to light yellowish color indicating the catalyst deactivation. Significant amount of coke was deposited on the catalyst with the made-up fraction when compared to the pyrolysis condenser fraction. We are currently working to investigate the long term stability of the catalyst as well as to minimize the coke formation in the continuous flow reactor.

One way of processing aqueous wastes containing sugars by minimizing char/coke formation and achieving complete carbon to gas conversion with high hydrogen selectivities is to first do a pretreatment step by catalytic hydrogenation at lower temperatures (300 °C), thereby converting all the sugars to respective polyols, which are then in a subsequent step comparatively easy to reform with much lesser operating problems than the original sugar compounds. Part of the hydrogen generated at high pressures from the reforming of polyols can be used for the catalytic hydrogenation step [1].

3.9. Catalyst characterization results

Thermo-gravimetric analysis of the internal coke deposited on the catalysts having different supports is shown in Fig. 12. Very less or almost no internal coke deposition on the γ-Al_2O_3 supported catalyst is noticed. The internal coke deposited on the activated carbon supported catalyst could not be quantified as the support started

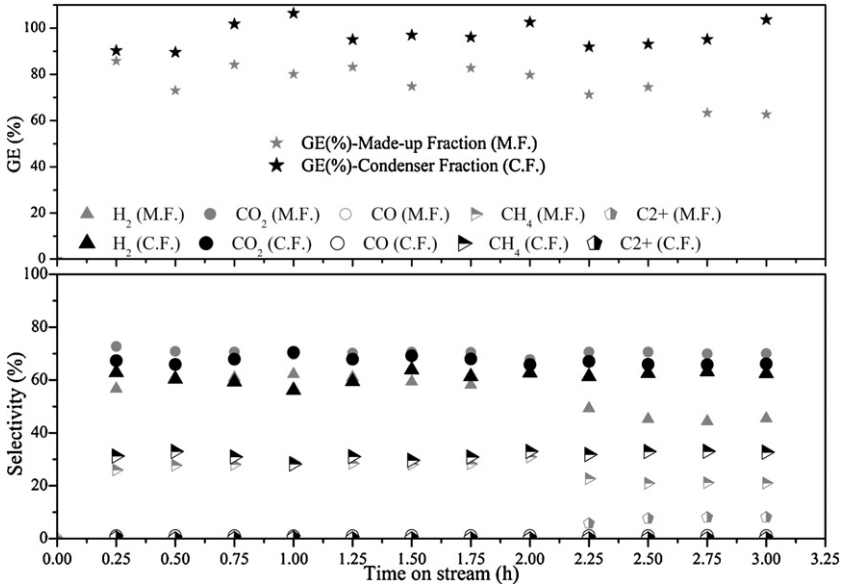

Fig. 11. Catalytic reforming of the aqueous fraction of bio-oil in supercritical water using a continuous flow reactor (experimental conditions: feed – Made-up-I and pyrolysis condenser fraction, feed concentration – 5 wt%, *T* – 600 °C, P – 250 bar, Ru/Ce–ZrO_2 catalyst – 6 g, flow – 2 ml/min).

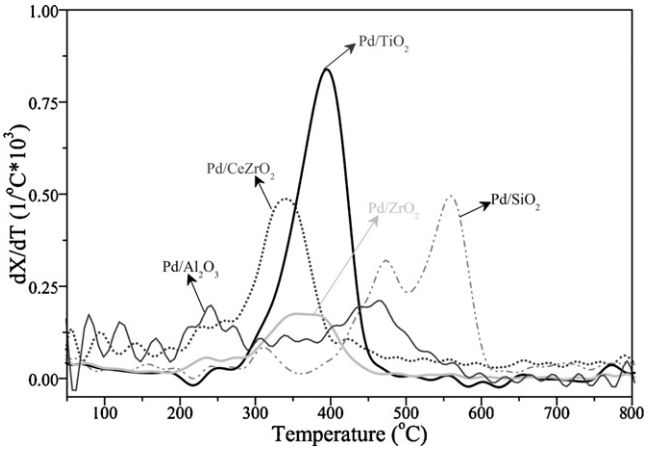

Fig. 12. Thermo-gravimetric analysis of the internal coke deposited on the spent catalysts (support effect: batch autoclave tests) after the reaction at heating rate of 10 °C/min in stream of flowing air (30 ml/min).

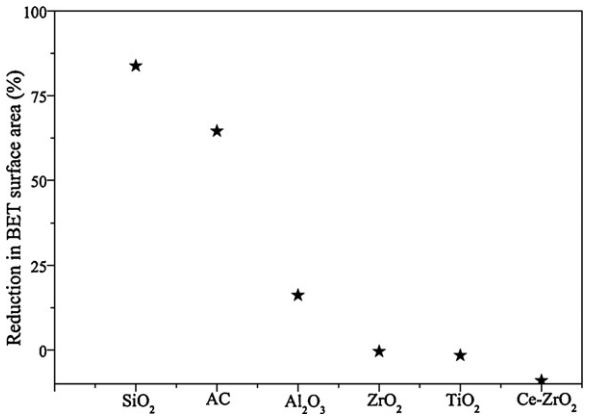

Fig. 14. Percentage reduction of catalyst surface area loss after 15 min of reaction time (support effect: batch autoclave results).

to completely oxidize in the temperature range of 400–700 °C. Maximum internal coke formation is observed with Ti supported catalysts. It is evident from Fig. 12, that two different cokes are formed on the support with respect to their characteristics. Low temperature coke conversion in the range of 300–450 °C is observed for TiO_2, Ce–ZrO_2 and ZrO_2 supported catalysts. Comparatively, high temperature coke conversion ranging from 400 to 600 °C is seen with silica supported catalysts.

The crystalline structures of the fresh and spent catalysts are verified by XRD analysis and are shown in Fig. 13. As can be seen from the figure, fresh γ-Al_2O_3 has two peaks at $2\theta = 45.8°$ and 66.8°. However, XRD spectra of the spent alumina catalysts revealed no phase changes as these experiments were carried out in a batch autoclave reactor for a short period or reaction time. The transformation of γ-Al_2O_3 increases with increasing temperature to corundum followed by a sequence of $\gamma \rightarrow \delta \rightarrow \theta \rightarrow \alpha$, the surface area decreases with each step and the final transition to the alpha phase is associated with the greatest decrease [34]. Elliott et al. [29,30] have reported that after the exposure of γ-Al_2O_3 in sub or supercritical water at 350 °C and 200 bar, δ- and γ-Al_2O_3 were completely hydrolyzed to give boehmite, while η-Al_2O_3 formed a mix of boehmite and α-Al_2O_3 leading to loss of surface area. In our earlier work, we have also presented similar observations of phase change and instability of alumina support in a continuous flow reactor for the reforming of ethylene glycol in supercritical water [22]. However, in this study we do not see such phase change of γ-Al_2O_3 (Fig. 13b) and this can be due to the experimental conditions used like type of reactor and reaction time. XRD analysis verified that the fresh Ti support was found in a mix of both rutile and anatase form and ZrO_2 support was found in monoclinic phase. Several unidentified peaks were noticed in the case of carbon supported spent catalyst after the reaction and we believe that this could be either due to phase change or the presence of contaminants.

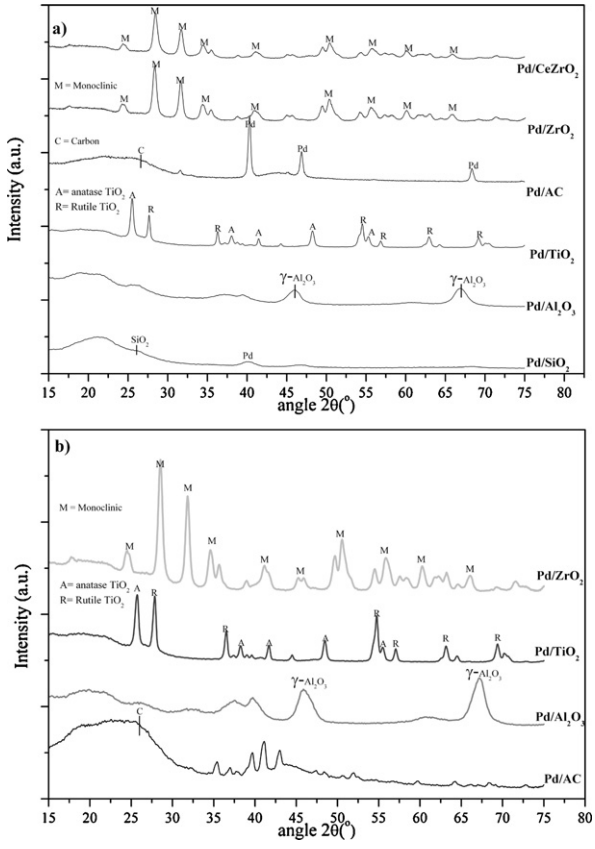

Fig. 13. XRD analysis of the fresh (a) and spent catalysts (support effect: batch autoclave tests) (b).

The loss in surface area due to phase change is shown in terms of BET surface area reduction is illustrated in Fig. 14. The percentage reduction of the BET surface area is defined as the ratio of final surface area after the reaction to the initial surface area. Significant loss in the surface area is observed for silica and activated carbon supports. A slight increase in the surface area of the catalyst is noticed with ZrO_2, TiO_2 and Ce–ZrO_2 after the reaction. This additional gain in the surface area after the reaction can be associated due to the deposition of internal coke in the catalyst. However, these changes in surface area reduction after the reaction may differ in realistic conditions when tested in a continuous flow reactor and also depends on the duration of the run. Based on the above mentioned observations, the stable supports identified for hydrothermal gasification of biomass include titania, zirconia and modified zirconia (Ce–ZrO_2), which are in agreement with literature [31].

Leaching of metals under hydrothermal conditions is another important issue that needs to be addressed by studying long duration tests in a continuous flow reactor. However, in this study based on the elemental analysis of the liquid and catalysts samples we did not notice any metal leaching and this can probably be due to very short reaction times.

4. Conclusions

Catalytic supercritical water gasification is an attractive process to processing wet biomass streams but also appears to be applicable for wastewater treatment produced from biomass pyrolysis and upgrading processes in a wood-based (ligno-cellulosic) biorefinery system. The main scope of this process is to completely convert the organics present in the water soluble fraction of bio-oil to combustible gases in the presence of a catalyst. The present study provides quantitative evaluation of the reforming activity of several catalysts, support materials and different operating parameters on the conversion and product gas selectivities of water soluble fraction of bio-oil. Ru was found to be the most active catalyst in terms of gasification efficiency as well as alkane selectivity.

The catalyst supports tested had a negligible effect on the conversion, but a prominent effect on the product gas distribution. Titania supported catalysts were found to have a high amount of internal char deposition when compared to other supports. Though carbon supported catalysts have high specific surface area they are more prone to gasify in the supercritical water. Stable support materials identified for the hydrothermal gasification of biomass include ZrO_2, Ce–ZrO_2 and TiO_2. High temperatures, low feedstock concentrations, high catalyst loadings and longer residence time favored high conversion. The aqueous wastewater from the HDO process was more easily converted than the aqueous fraction obtained from the condenser fraction and the made-up waste stream. Complete GE with stable product gas selectivities were obtained with the condenser fraction when compared to the made-up fraction and this significant difference between the two feedstocks is primarily due to the presence of sugars components in the made-up fraction which lead to coke formation and incomplete conversion due to catalyst deactivation.

Acknowledgement

This project was funded by the EOS-LT program of SenterNovem (EOS-LT 05020).

References

[1] T.P. Vispute, G.W. Huber, Green Chemistry 11 (2009) 1433.
[2] J.M.L. Penninger, M. Rep, International Journal of Hydrogen Energy 31 (2006) 1597.
[3] A.G. Chakinala, D.W.F. Brilman, W.P.M. van Swaaij, S.R.A. Kersten, Industrial & Engineering Chemistry Research 49 (2010) 1113.
[4] M.H. Waldner, F. Vogel, Industrial & Engineering Chemistry Research 44 (2005) 4543.
[5] J.M.L. Penninger, G.J.J. Maass, M. Rep, International Journal of Hydrogen Energy 32 (2007) 1472.
[6] M.H. Waldner, F. Krumeich, F. Vogel, Journal of Supercritical Fluids 43 (2007) 91.
[7] A.J. Byrd, S. Kumar, L.Z. Kong, H. Ramsurn, R.B. Gupta, International Journal of Hydrogen Energy 36 (2011) 3426.
[8] R.P. Balegedde Ramachandran, G. van Rossum, W.P.M. van Swaaij, S.R.A. Kersten, Energy & Fuels 25 (2011) 5755.
[9] R.P.B. Ramachandran, G. van Rossum, W.P.M. van Swaaij, S.R.A. Kersten, Environmental Progress & Sustainable Energy 28 (2009) 410.
[10] F. De Miguel Mercader, P.J.J. Koehorst, H.J. Heeres, S.R.A. Kersten, J.A. Hogendoorn, AIChE Journal 57 (2011) 3160.
[11] C. Di Blasi, C. Branca, A. Galgano, D. Meier, I. Brodzinski, O. Malmros, Biomass and Bioenergy 31 (2007) 802.
[12] S. Idesh, S. Kudo, K. Norinaga, J.-I. Hayashi, Energy & Fuels 26 (2012) 67.
[13] R.J.M. Westerhof, D.W.F. Brilman, M. Garcia-Perez, Z. Wang, S.R.G. Oudenhoven, W.P.M. van Swaaij, S.R.A. Kersten, Energy & Fuels 25 (2011) 1817.
[14] R.J.M. Westerhof, D.W.F. Brilman, W.P.M. van Swaaij, S.R.A. Kersten, Industrial & Engineering Chemistry Research 49 (2009) 1160.
[15] F. De Miguel Mercader, Pyrolysis oil upgrading for co-processing in standard refinery units, Thermochemical Conversion of Biomass, Vol. PhD Thesis, University of Twente, Enschede, 2010, p. 176.
[16] R.J.M. Westerhof, Refining Fast Pyrolysis of Biomass, University of Twente, Enschede, 2011.
[17] R.J.M. Westerhof, N.J.M. Kuipers, S.R.A. Kersten, W.P.M. van Swaaij, Industrial & Engineering Chemistry Research 46 (2007) 9238.
[18] B.G. Kyle, Prentice Hall PTR, Englewood cliffs, New Jersey, 1999.
[19] G. Soave, M. Barolo, A. Bertucco, Fluid Phase Equilibria 91 (1993) 87.
[20] A. Bertucco, M. Barolo, G. Soave, Industrial & Engineering Chemistry Research 34 (1995) 3159.
[21] S. Giorgio, Chemical Engineering Science 27 (1972) 1197.
[22] D.J.M. de Vlieger, A.G. Chakinala, L. Lefferts, S.R.A. Kersten, K. Seshan, D.W.F. Brilman, Applied Catalysis B: Environmental 536 (2012) 111–112.
[23] R.R. Davda, J.W. Shabaker, G.W. Huber, R.D. Cortright, J.A. Dumesic, Applied Catalysis B: Environmental 43 (2003) 13.
[24] R.R. Davda, J.W. Shabaker, G.W. Huber, R.D. Cortright, J.A. Dumesic, Applied Catalysis B: Environmental 56 (2005) 171.
[25] K.G. Azzam, I.V. Babich, K. Seshan, L. Lefferts, Journal of Catalysis 251 (2007) 163.
[26] T. Minowa, T. Ogi, Catalysis Today 45 (1998) 411.
[27] W. Ruettinger, X. Liu, R.J. Farrauto, Applied Catalysis B: Environmental 65 (2006) 135.
[28] A. Wootsch, C. Descorme, D. Duprez, Journal of Catalysis 225 (2004) 259.
[29] D.C. Elliott, Biofuels Bioproducts & Biorefining-Biofpr 2 (2008) 254.
[30] D.C. Elliott, L.J. Sealock Jr., E.G. Baker, Industrial and Engineering Chemistry Research 32 (1993) 1542.
[31] D.C. Elliott, T.R. Hart, G.G. Neuenschwander, Industrial and Engineering Chemistry Research 45 (2006) 3776.
[32] A. Nakamura, E. Kiyonaga, Y. Yamamura, Y. Shimizu, T. Minowa, Y. Noda, Y. Matsumura, Journal of Chemical Engineering of Japan 41 (2008) 817.
[33] J.A.M. Withag, J.R. Smeets, E.A. Bramer, G. Brem, The Journal of Supercritical Fluids 61 (2012) 157.
[34] A.J. Byrd, R.B. Gupta, Applied Catalysis A: General 381 (2010) 177.